Ionization efficiency due to primary and secondary photoelectrons : A numerical model

J. LILENSTEN ([1]), W. KOFMAN ([1]), J. WISEMBERG ([2]), E. S. ORAN ([3]), and C. R. DEVORE ([3])

([1]) *CEPHAG, URA* 322, *INPG/IEG, BP* 46, *F*-38402 *St Martin d'Hères Cedex, France*
([2]) *Institut d'Aéronomie Spatiale,* 3, *av. Circulaire, B* 1180, *Bruxelles, Belgique*
([3]) *Laboratory for Computational Physics and Fluid Dynamics, Naval Research Laboratory, Washington, D.C.* 20375, *USA*

Received May 19, 1988 ; revised July 17, 1988 ; accepted July 29, 1988.

ABSTRACT. In the ionosphere, the EUV solar flux ionizes the neutral gas, producing a primary distribution of electrons. These primary electrons may have sufficient energy to produce new secondary electrons, by inelastic collisions with neutrals. We define the efficiency of this production by the ratio between the secondary and the primary production. Computation of this efficiency for different solar conditions shows that it is approximately constant above 200 km, varying from 12 % with a quiet sun to 22 % with a disturbed sun at 500 km. It increases drastically in the *E*-region reaching a peak value of 2 to 3, (between 120 and 150 km, depending on the intensity of the solar flux, and the solar zenith angle). Influences of solar zenith angle, altitude and latitude on the ionization efficiency are studied. A simple model is described that allows easy computation of the secondary production.

Annales Geophysicae, 1989, **7,** (1), 83-90.

INTRODUCTION

Using the detailed spectral information on the extreme ultraviolet solar flux at wavelengths capable of ionizing the major thermospheric constituents (< 102.7 nm) that is available, (Hinteregger *et al.*, 1973 ; Torr and Torr, 1979), the rate of primary electrons produced by ionization due to this flux has been computed (Torr *et al.*, 1979 ; Torr and Torr, 1985). Secondary ionization occurs by collisions between the energetic primary electrons and the neutral particles. The electrons are then transported in the ionosphere, and degraded by ionization, excitation, and energy losses to heat the ionosphere.

This secondary production has been computed by a number of different approaches (Nagy and Banks, 1970 ; Mantas, 1975 ; Strickland *et al.*, 1976 ; Schunk and Nagy, 1978 ; Stamnes, 1980), all of which solve a complicated transport equation. However, in many ionospheric modelling efforts, no such detailed photoelectron transport equations are solved and the secondary ionization is then often assumed to be 30 % of the primary (Roble *et al.*, 1987). This approximation is very rough, and more accurate estimates are required.

We describe in this paper a calculation of the ionization efficiency as a function of the solar EUV flux, the solar zenith angle, latitude and altitude. First, the equations for primary and secondary production are presented, and the photoelectron efficiency is theoretically introduced. Then, we study variations in this efficiency and propose a simple way to model it.

THEORETICAL BACKGROUND

In the terrestrial ionosphere, the EUV solar flux (< 102.7 nm) produces electrons by ionization of neutral particles. These « primary » electrons move along the magnetic field, producing heating, excitation and ionization (« secondary » electrons). The transport equation that describes the production of electrons governs the evolution of a steady-state electron flux from the top of the ionosphere to the low *E*-region. Under certain approximations, this equation can be written in a relatively simple form : First, we assume that photoelectrons are transported predominantly along magnetic field lines, and that the atmosphere is perpendiculary stratified along these field lines. This approximation is good at middle and high latitudes. Second, motions perpendicular to the magnetic field are neglected. Third, we assume no electric fields are present. Under these assumptions, the transport equation can be written (Oran and Strickland, 1978) as :

$$\mu \frac{\partial \Phi(\tau, \mu, E)}{\partial \tau(z, E)} = -\Phi(\tau, \mu, E) + sf(\tau, \mu, E) + \frac{n_e(z)}{\sum_k n_k(z) \cdot \sigma_k^T(E)} \cdot \frac{\partial}{\partial E}(L(E) \cdot \Phi(\tau, \mu, E)) +$$

$$+ \sum_\ell \left[\frac{n_\ell(z) \cdot \sigma_\ell^T(E)}{\sum_k n_k(z) \cdot \sigma_k^T(E)} \int_{-1}^{1} d\mu' \int_E^{E_{max}} dE' R^\ell(E' \mu' \rightarrow E, \mu) \Phi(\tau, E', \mu') \right] \quad (1)$$

$\Phi(\tau, \mu, E)$ = Photoelectron stationary flux ($cm^{-2} s^{-1} eV^{-1} sr^{-1}$).
E, E' = Energies (eV) of scattered and incident electrons.
μ, μ' = Cosines of scattered and incident electron pitch-angle.
$\tau(z, E)$ = Electron scattering depth, defined by :

$$d\tau(z, E) = \sum_k \sigma_k^T(E) n_k(z) dz .$$

R^ℓ = Redistribution function describing the degradation from a state (E', μ') to a state (E, μ) for the neutral species ℓ (O, O_2, N_2).
$\sigma_k^T(E)$ = Total elastic and inelastic collision cross section for the neutral species k, for one electron at energy E.
$n_k(z)$ = Density of the neutral species k (O, O_2, N_2) determined from a neutral atmosphere model. The MSIS model was used.
$n_e(z)$ = Electron density.

• The left-hand part of the equation $\mu \frac{\partial \Phi(\tau, \mu, E)}{\partial \tau(z, E)}$ is the steady-state flux $\Phi(\tau, \mu, E)$ variation with the scattering depth.

• The second term on the right-hand side of the equation is the primary photo-electron production rate (in units of $cm^{-2} s^{-1} eV^{-1} sr^{-1}$) caused by solar EUV :

$$sf(\tau, \mu, E) = \frac{1}{4\pi \sum_k n_k(z) \cdot \sigma_k^T(E)} q_{k,i}(z, W) \quad (2)$$

$$q_{k,i}(z, W) = n_k(z) \cdot \sigma_{k,i}^{ion}(E) \Phi_\infty(E) \times$$
$$\times \exp\left\{ - \sum_m \sigma_m(E) \cdot \int_z^{+\infty} n_m(s) ds \right\} \quad (3)$$

$q_{k,i}$ = Primary electron production ($cm^{-3} s^{-1} eV^{-1}$).
W = $E - I_{k,i}$, where $I_{k,i}$ is the ionization threshold for species k, at the i-th state.
$\sigma_{k,i}^{ion}$ = Ionization cross section for species k, at the i-th state.
Φ_∞ = Solar flux on the top of the ionosphere.
$\sigma_m(E)$ = Absorption cross section of the neutral species m for one photon at energy E.

The integration is done along s, the line of sight to the sun. To obtain the primary production along a vertical column, a Chapman function was used, which is a function of the solar zenith angle χ.

The third term on the right side, $n_e(z) \frac{\partial}{\partial E}(L(E) \cdot \Phi(\tau, \mu, E))$, represents the losses due to frictional processes (collisions between photo-electrons and thermal-electrons), equal to $-n_e(z) L(E) \left(\frac{\Phi(\tau, \mu, E)}{E} - \frac{\partial \Phi(\tau, \mu, E)}{\partial E} \right)$. The stopping cross section $L(E)$ is described in Oran and Strickland (1978). Frictional processes become important at low energies (less than the ionization threshold), and do not influence the secondary electron production.

The last term represents the electron production due to degradation of higher-energy fluxes (collisions between photoelectrons and neutral particles) (Mantas, 1973 ; Oran and Strickland, 1978 ; Stamnes, 1981).

The primary electron production can be found by integrating q_{ki} in

$$P_p(z) = \int q_{ki}(z, E - \ell_{k,i}) dE . \quad (4)$$

The secondary electron production is deduced from (1) as :

$$P_s(z) = \sum_m n_m(z) 2\pi \int_{-1}^{1} d\mu \times$$
$$\times \int_{e_{min}}^{e_{max}} dE \sigma_m^{ion}(E) \cdot \Phi(z, E, \mu) \quad (5)$$

which lead us to define the *primary electron ionization efficiency* as :

$$K_L(z) = \frac{P_s(z)}{P_p(z)} . \quad (6)$$

RESULTS

Electron production

The programs solving (1) and (3) are described in Strickland *et al.* (1976), and Oran and Strickland

(1978). These programs work on three different grids : One is for altitude, the second for energy and the third is an angular grid, that is used to determine the angular distribution of scattered electrons. As long as we are not interested in the angular distribution function, we may consider only two streams. The neutral atmosphere model MSIS 83 was implemented (Hedin *et al.*, 1977), in place of the Jacchia 77 model used by Oran and Strickland.

In the present version, we implemented the solar EUV flux measurements obtained from the Atmosphere Explorer satellites during solar minimum and maximum conditions (Hinteregger, 1981 ; Hinteregger and Katsura, 1981). The values used are those parameterized and modified by Torr and Torr (1985), into 37 energy values from 248 to 12.02 eV (17 discrete solar EUV lines and 20 energy intervals, with averaged fluxes). Photoionization, dissociative photoionization and photoabsorption cross sections, are taken from Kirby *et al.* (1979).

Photoelectron collision cross sections are taken from Blaha and Davis (1975) for O. The values of Shyn *et al.* (1972) have been used for N_2. The O_2 values have been obtain from Tramjar *et al.* (1972), Watson *et al.* (1967), and Dehmel *et al.* (1976). This set has been discussed in Oran and Strickland (1978), and is very close from Green and Stolarski values (1972). Stamnes and Rees (1983) studied the effects that some composite sets of inelastic cross section would have on electron energy deposition, and electron heating rate. They compared Green and Stolarski's data, Victor's data and Pitchford and Phelps' data, concluding that « the choice of cross section sets does not seem important » in resolving the electron transport equation.

We considered the variation of the efficiency with different parameters : Altitude, solar zenith angle and latitude. The solar zenith angle is a function of hour, declination and latitude. Thus, the latitude influences the results through changes in the solar zenith angle.

But the neutral atmosphere is also influenced by the latitude. Then, we considered latitude as an independent parameter. We computed the efficiency for 9 latitudes (from 45 to 84 degrees), 13 solar zenith angles at each latitude, and on an altitude grid of 41 values between 100 and 500 km. The photoelectron calculation was truncated at 3 eV. Our computations were done for 3 solar fluxes : The two cited above

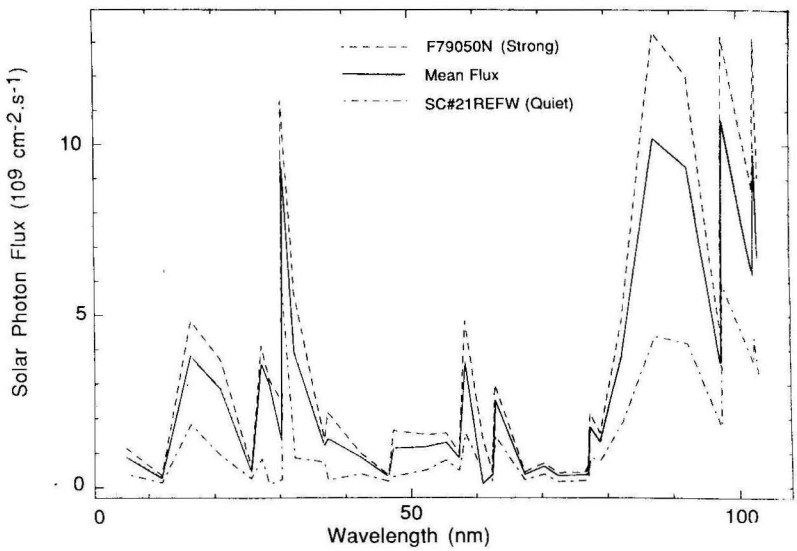

Figure 1
Three solar fluxes used in this paper. F79050N *and* SC # 21REFW *are the fluxes for strong and quiet solar conditions respectively, as referenced by Hinteregger, and modified by Torr and Torr (see text).*

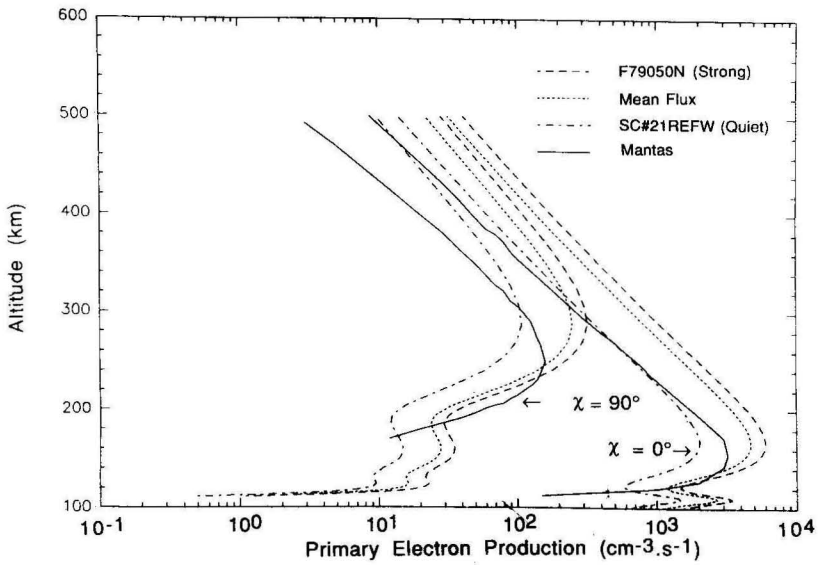

Figure 2
Primary electron production for the three solar conditions for solar zenith angles of 90° *and* 0°.

which are a quiet solar flux ($f_{10.7} = 68$), referenced as SC#21 REFW, and a strong solar flux ($f_{10.7} = 243$), referenced as F79050N by Hinteregger (1981). A third flux was created, which is simply the arithmetic average of the quiet and the strong one, to obtain results concerning mean conditions ($f_{10.7} = 155$) (fig. 1).

Calculated primary electron production (eq. (4)) for minimum and maximum zolar zenith angle, is shown in figure 2, and compared to those obtained by Mantas (1973) for the same exospheric temperature. The differences are due to the different solar fluxes, and to the model of atmosphere used. Compared to the MSIS model used in this study, the Jacchia model used by Mantas underestimates the atomic oxygen density at high altitude. This leads to a decrease in the altitude of maximum of production. The peak around 110 km is due to the high-energy spectral radiation interval at 186 eV and to intense low energy lines, as 12.11 or 12.69 eV, whose energies are less than the ionization threshold for O (13.62 eV) and N_2 (15.62 eV). These spectral lines have an effect at low altitudes, were O_2 is abundant. The effect of different discrete wavelengths is shown figure 3.

The secondary production (eq. (5)) is shown figure 4 (thin lines), and compared to primary production (heavy lines). A local maximum occurs for the secondary production at altitudes less than 200 km where the production is local and the primary production is large. The maximum secondary electron production occurs at lower altitudes (around 105 km).

To judge and control the accuracy of the solutions of transport equation, we computed the energy conservation by calculating the elements of the equation (Swartz, 1985) :

$$\int_{e_{\min}}^{e_{\max}} \mathrm{d}E \cdot E \cdot \int_{-1}^{1} \mathrm{d}\mu \cdot \sum_{\ell} n_\ell(z) \cdot \sigma_\ell^T(E) \cdot sf(z, \mu, E) =$$

$$\int_{e_{\min}}^{e_{\max}} \mathrm{d}E \cdot n_e(z) \cdot L(E) \int_{-1}^{1} \mathrm{d}\mu \; \Phi(z, E, \mu) + \int_{e_{\min}}^{e_{\max}} \mathrm{d}E \cdot \sum_{\ell} n_\ell(z) \cdot \sigma_\ell^j(E) \cdot I_j \cdot \int_{-1}^{1} \mathrm{d}\mu \; \Phi(z, E, \mu) \,. \qquad (7)$$

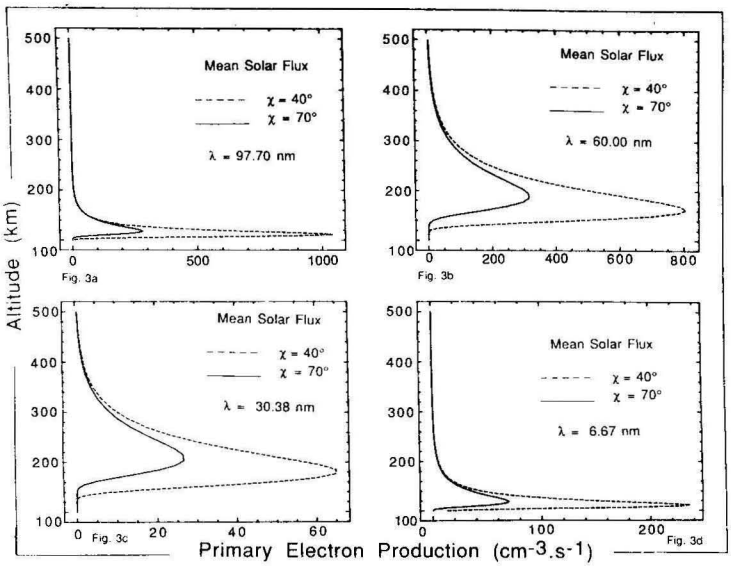

Figure 3

The altitude production due to selected discrete solar EUV lines (6.67, 30.38, 60.0 *and* 97.70 nm), *shown for mean conditions, at two different solar zenith angles. Intense low-energy lines and high-energy lines create the local maximum of primary production at* 110 km.

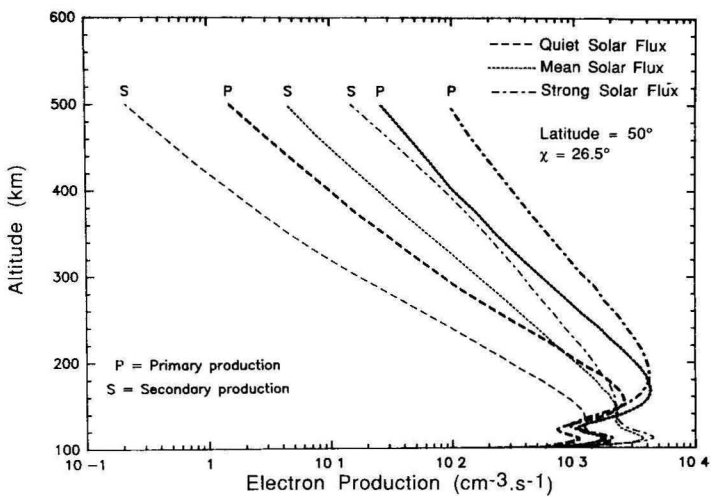

Figure 4

Primary and secondary electron production for the three solar conditions, at a latitude 50°, *and solar zenith angle* 26.5°.

This is equivalent to saying that the first energy moment of the primary production rate equals the rate of energy deposition in all excitation and heating processes. For the 3 fluxes (quiet, mean, strong), the relative difference between the left and the right side of the equation are 2.53 %, 1.50 %, 1.8 % respectively.

Efficiency K_L

We studied the efficiency variation as a function of the solar flux, latitude, solar zenith angle and altitude. In the neutral atmosphere model, the a_p geomagnetic index used is 21 and the longitude is fixed at 0°. To study the efficiency at different solar zenith angles, it was necessary to run the programs for different dates at high latitudes. For example, at a latitude of 85°, the minimum solar zenith angle (61.5°) is reached at the 173rd day. But at this date, the highest solar zenith angle is 71.5°, far from our maximum (84°, reached before the 110th day). The effect of changing the date is essentially to change the O density. This is unimportant at low altitudes, were the efficiency is high, and does not affect the values at high altitudes, where the efficiency is approximately constant. Therefore, the date was not considered as a meaning parameter. The exospheric temperature computed by the model is 1162 K.

Figure 5 shows the effect of different parameters on the efficiency for quiet conditions. The variation of K_L with altitude is shown (fig. 5*a*) for several values of the solar zenith angle. One can see that above the *E*-region, the efficiency is approximately constant, varying from 15 % to 40 % between 200 and 500 km for quiet, mean and strong solar conditions, and is independent of latitude or solar zenith angle (see also figs. 7*a* and 7*b*).

In the *E*-region, K_L increases drastically to reach a value greater than 2 in quiet conditions, and greater than 3 for strong solar flux. K_L increases further with the solar zenith angle. Increasing the solar zenith angle from 26.5° to 72.2° increases the maximum efficiency by a factor 1.10, 1.16 and 1.27 for quiet, mean and strong conditions, respectively. This also affects the height of the maximum of efficiency, which increases from 118 km to 140 km approximately (fig. 5*c*), and on the amplitude of the maximum of efficiency (fig. 5*d*). The increase in altitude of maximum efficiency can be attributed to the fact that the atmosphere at low altitudes is first in dusk when χ increases. The enhancement of the efficiency can be explained by the fact that the photo-absorption cross section is high between 30 and 80 nm for atomic oxygen, which is abundant at high altitudes. When the sun is low (large zenith angles), photons are crossing a larger part of ionosphere than for small zenith angle conditions. There is more EUV absorption in this case (between 30 and 80 nm) than at the extreme energies of the spectrum. There are fewer primary electrons created, but high-energy primary electrons are less affected. The result is that P_s does not decrease as much as P_p, and the efficiency is higher.

The variation of the efficiency with respect to the solar zenith angle, at a given altitude of 106 km, is shown (fig. 5*b*) for 4 different latitudes. At this low altitude and at a given solar zenith angle, an increase of the latitude makes the efficiency increase. For example, at a solar zenith angle of 70°, K_L is approximately 0.5 for a latitude of 45°, and 0.85 at 75°. The reason is the same than above, since at low altitudes, the atomic oxygen becomes higher at low latitude than at high latitude for the same solar zenith angle. This effect tends to disappear when altitude becomes higher. One can see (figs. 5*c* and 5*d*) that there is a small effect of the latitude on the variation of the altitude or amplitude of the maximum efficiency.

MODEL FOR THE SECONDARY ELECTRON PRODUCTION

A general model for computing the secondary electron production, available for all solar conditions, requires an accurate model for representing the EUV variability in terms other than those based on EUV parameters, such as the solar radio emission at 2800 MHz ($f_{10.7}$) (Hintereger, 1981). Here, we propose a model with three sets of coefficients for the three solar

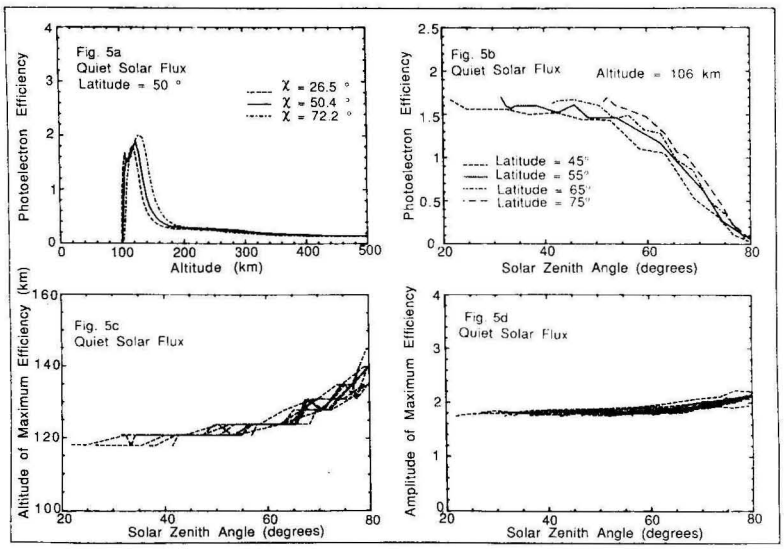

Figure 5
Variation of the efficiency in quiet solar conditions at four latitudes with (a) *altitude,* (b) *solar zenith angle. Figures 5c and 5d show the variation of the altitude and amplitude of the maximum efficiency, 9 latitudes.*

conditions. The process consists of determining the altitude z_m of the maximum efficiency, the corresponding amplitude A, and fitting the efficiency to :

$$K_L^{\text{est}} = A(\chi) \exp\left(-\left(\frac{z - z_m(\chi)}{\sigma}\right)^{2\alpha_1}\right) \quad \text{if} \quad z \leqslant z_m \quad (8)$$

$$K_L^{\text{est}} = (A(\chi) - C) \exp\left(-\left(\frac{z - z_m(\chi)}{\sigma}\right)^{2\alpha_2}\right) + C \quad \text{if} \quad z > z_m , \quad (9)$$

where K_L^{est} is the estimated efficiency, C is a constant (threshold efficiency for high altitudes, depending only on the solar activity), A and z_m are function of the solar zenith angle, and latitude :

$$A = \frac{\alpha_3}{\cos(\chi)} + \alpha_4 + \alpha_5 \sin(\text{latitude})$$

$$z_m = \frac{\alpha_6}{\cos(\chi)} + \alpha_7 + \alpha_8 \sin(\text{latitude}) .$$

Coefficients to compute A, z_m and K_L^{est} are summarized in table 1, and their use is shown (fig. 6) for quiet conditions. The coefficients were adjusted by minimizing the sum of squares of the function $(K_L - K_L^{\text{est}})$.

Table 1

Coefficients for computing the secondary electron production (eq. (8) and (9)).

Flux	Quiet	Mean	Strong
α_1	0.721	0.680	0.665
α_2	2.30	1.53	1.36
α_3	0.088	0.156	0.209
α_4	2.05	2.79	3.52
α_5	− 0.43	− 0.59	− 0.86
α_6	4.61	5.73	6.28
α_7	118	116	120
α_8	− 4.54	− 2.71	− 4.31
σ	21.1	21.6	22.1
C	0.223	0.303	0.364

The mean error between the full calculation and the model is about 5 %.

To show the results of the model for strong and mean solar conditions, comparisons between computed and modelled efficiencies are shown (fig. 7) at a latitude 50°. As in figures 5*a* and 6*a*, we show the efficiency as a function of altitude, for the same three solar zenith angles.

The threshold efficiency at high altitudes has been determined by minimizing the sum of squares. For

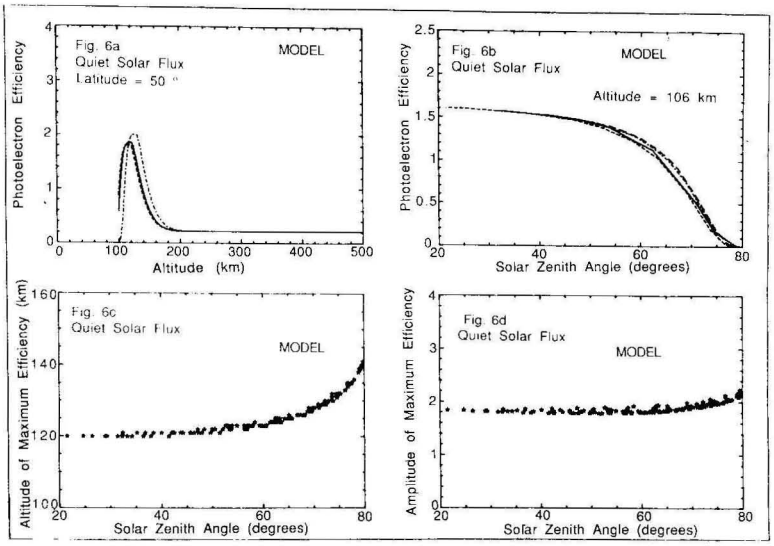

Figure 6

Modelled efficiency in quiet solar conditions corresponding to the same conditions as figure 5.

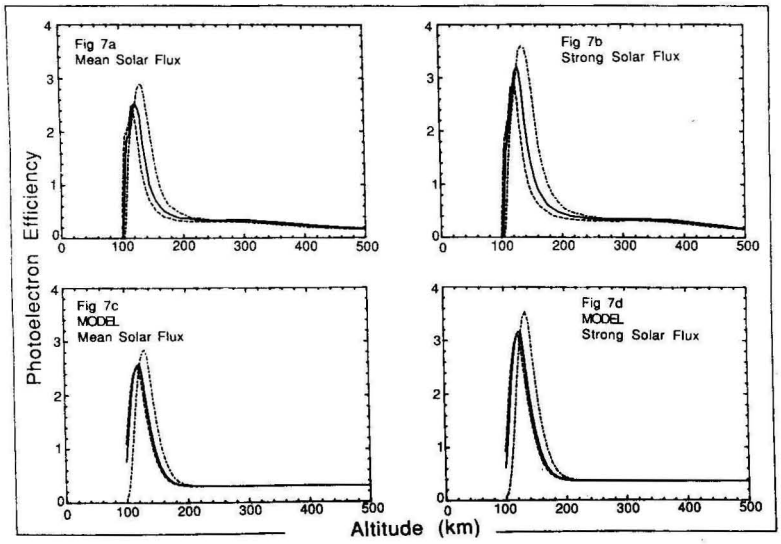

Figure 7

Variation of the efficiency with altitude for strong and mean conditions (figs. 7a and 7b). The results of the simplified model are shown in figures 7c and 7d. The three lines correspond to the same solar zenith angle as on figures 5a and 6a.

quiet, mean and strong conditions, it is 21.5 %, 30.3 % and 36.4 % respectively. Therefore, the value used by Roble *et al.* (1987) (30 %) was a good estimate of the threshold.

The model does not very accurately fit the computed value of the efficiency at 100 km. This height is the limiting value at low altitudes for this study. To calculate the secondary production, the program computes at each altitude an upward and a downward stationary flux. At this 100 km limit, the downward secondary production is lost and the efficiency is not very realistic. Therefore, it is unimportant to match the shape of the curve.

The influence of the solar zenith angle is very well reproduced when considering an approximation $(1/\cos(\chi))$ of the Chapman function. This is not surprising, since the Chapman function is used directly in the primary production equation in the main calculation.

CONCLUSION

Models to compute parameters on the global structure of the ionosphere need an accurate estimation of the electron production (Taïeb and Poinsard, 1984). Currently, the primary production is computed directly, and then, the total electron production is deduced from the primary by simply using a growth factor (1.3 in Roble, 1987). According to this study, in the *F*-region, this fudge factor is a good average value, for the efficiency K_L, defined as the ratio between secondary and primary electron production, for mean solar conditions. In the *E*-region, the secondary production can be 2 or 3 times the primary one. We have presented a model which allows an estimation of the secondary production, as a function of the altitude, latitude and solar zenith angle, provided that the primary production is known (eq. (3)). The average error between the efficiency computed by solving the transport equation or by the simple model is less than 5 %. We have determined coefficients of this model for three different solar conditions.

In a recent paper (Richard and Torr, 1988), a parallel study was published. The study was done for a single solar zenith angle (instead of 117 in this study). The bottom altitude was 120 km (100 km in this work), and they truncated the photoelectron calculation at 100 eV (248 in the present work). The secondary production was studied for the separate elements of the atmosphere. These differences make the comparison with our study difficult.

However, the authors founded also a good agreement with the value of 1.3 used for previous aeronomic calculations, and pointed out that the efficiency cannot be represented by constant at low altitude.

Acknowledgements

Helpful discussions with Dr. V. Wickwar, and with Dr. G. Kockarts are gratefully acknowledged.

REFERENCES

Banks, P. M., and G. Kockarts, *Aeronomy,* part A and B, Academic Press, 1973.

Blaha, M., and J. Davis, Elastic scattering of electrons by oxygen and nitrogen at intermediate energies, *Phys. Rev.*, **12,** 2319-2324, 1975.

Dehmel, R. C., M. A. Fineman, and D. R. Miller, Angular scattering of low energy electrons by atomic and molecular oxygen, argon and helium, *Phys. Rev.*, **13,** 115-122, 1976.

Green, A. E. S., and R. S. Stolarski, Analytic models of electron impact excitation cross section, *J. Atmos. Terr. Phys.*, **34,** 1703-1717, 1972.

Hedin, A. E., J. E. Salah, J. V. Evans, C. A. Reber, G. P. Newton, N. W. Spencer, D. C. Kayser, D. Alcaydé, P. Bauer, L. Cogger and J. P. McClure, A global thermospheric model based on mass spectrometer and incoherent scatter data, *J. Geophys. Res.*, **82,** 2139-2156, 1977.

Hinteregger, H. E., Representation of solar EUV fluxes for aeronomical applications, *Adv. Space Res.*, **1,** 39-52, 1981.

Hinteregger, H. E., and F. Katsura, Observational, reference and model data on solar EUV, from measurements on AE-E, *Geophys. Res. Lett.*, **8,** 1147-1150, 1981.

Hinteregger, H. E., D. E. Bedo, and J. E. Manson, The EUV spectrophotometer on Atmosphere Explorer, *Radio Sci.*, **8,** 349-354, 1973.

Kirby, K., E. R. Constantinides, S. Babeu, M. Oppenheimer, and G. A. Victor, Photoionization and photoabsorption cross sections of He, O, and O_2 for aeronomic calculations, *Atmos. data and Nucl. Data Tables,* **23,** 63-81, 1979.

Mantas, G. P., Electron collision processes in the ionosphere, *Aeronomy report n° 54,* Aeronomy Laboratory, Dept. of electrical engineering, Univ. of Illinois, Urbana, Ill., 1973.

Mantas, G. P., Theory of photoelectron thermalization and transport in the ionosphere, *Planet. Space Sci.*, **23,** 337-354, 1975.

Nagy, A. F., and P. M. Banks, Photoelectron fluxes in the ionosphere, *J. Geophys. Res.*, **75,** 6260-6270, 1970.

Opal, C. B., W. K. Peterson, and E. C. Beaty, Measurement of secondary-electron spectra produced by electron impact ionization of a number of simple gases, *J. Chem. Phys.*, **55,** 4100-4106, 1971.

Oran, E. S., and D. J. Strickland, Photoelectron flux in the earth's ionosphere, *Planet. Space Sci.*, **26,** 1161-1177, 1978.

Richard, P. G., and D. G. Torr, Ratio of photoelectron to EUV ionization rate for aeronomic studies, *J. Geophys. Res.*, **93,** 4060-4066, 1988.

Roble, R. G., E. C. Ridley, and R. E. Dickinson, On the global mean structure of the thermosphere, *J. Geophys. Res.*, **92,** 8745-8758, 1987.

Rostoker, G., Geomagnetic indices, *Rev. Geophys. Space Phys.*, **10,** 935-950, 1972.

Shyn, T. W., R. S. Stolarski, and G. R. Carignan, Angular distribution of electrons elastically scattered from N_2, *Phys. Rev.*, **6,** 1002-1012, 1972.

Schunk, R. W., and A. F. Nagy, Electron temperature in the *F*-region of the ionosphere : Theory and observation, *Rev. Geophys. Space Phys.*, **16,** 355-399, 1978.

Stamnes, K., Analytic approach to auroral electron transport and energy degradation, *Planet. Space Sci.* **28,** 427-441, 1980.

Stamnes, K., On the two-stream approach to electron transport and thermalization. *J. Geophys. Res.*, **86,** 2405-2410, 1981.

Stamnes, K., and M. H. Rees, Inelastic scattering effects on photoelectron spectra and ionospheric electron temperature, *J. Geophys. Res.*, **88,** 6301-6309, 1983.

Strickland, D. J., D. L. Book, T. P. Coffey, and J. A. Fedder, Transport equation technique for the deposition of auroral electrons, *J. Geophys. Res.*, **81,** 2755-2764, 1976.

Swartz, W. E., Optimization of electron energy degradation calculation, *J. Geophys. Res.*, **90,** 6587-6593, 1985.

Taïeb, C., and P. Poinsard, Modelling of the mid-latitude ionosphere, *Ann. Geophysicae,* **2,** 197-206, 1984.

Torr, M. R., and D. J. Torr, Ionization frequencies for major thermospheric constituents as a function of solar cycle 21, *Geophys. Res. Lett.*, **6,** 771-774, 1979.

Torr, M. R., and D. J. Torr, Ionization frequencies for solar cycle 21 : Revised, *J. Geophys. Res.*, **90,** 6675-6678, 1985.

Torr, D. J., M. R. Torr, H. C. Brinton, L. H. Brace, N. W. Spencer, A. E. Hedin, W. B. Hanson, J. H. Hoffman, A. O. Nier, J. C. G. Walker, and D. W. Ruch, An experimental and theoretical study of the mean diurnal variation of O^+NO^+ and $N2^+$ ions in the mid latitude *F*1 layer of the ionosphere, *J. Geophys. Res.*, **84,** 3360-3372, 1979.

Tramjar, S., W. Williams, and A. Kupperman, Angular dependence of electron impact excitation cross section of O_2, *J. Chem. Phys.*, **56,** 3759-3765, 1972.

Watson, C. E., V. A. Jr. Dulock, R. S. Stolarski, and A. E. S. Green, Electron impact cross sections for atmospheric species. III, molecular oxygen, *J. Geophys. Res.*, **72,** 3961-3966, 1967.